International Journal of Research and Applied Innovations (IJRAI)

| ISSN: 2455-1864 | www.ijrai.org | editor@ijrai.org | A Bimonthly, Scholarly and Peer-Reviewed Journal |

||Volume 7, Issue 2, March–April 2024||

DOI:10.15662/IJRAI.2024.0702005

GEIOS EQG for Retrofit Wells: Repowering well with Advanced Metamaterials for Heat transfer and Advance Nano-Stimulation

Gerald Goorman[1], Sebastien Mollet[2], Marc Gelier Nathan[3], Sandra Brassier[4],

Shad Abdelmoumen SERROUNE[5], Dr. Khasani[6]

Head of Simulation and CFD at GEIOS Technologies, NANOGEIOS Laboratory and GEIOS Technologies (**00hbz7e82-Registered Lab**), USA[1]

Director of EQG Deployment and well Enhancement strategies, NANOGEIOS Laboratory and GEIOS Technologies (**00hbz7e82-Registered Lab**), USA[2]

Director of EQG Heat Transfer for NPC, NANOGEIOS Laboratory and GEIOS Technologies (**00hbz7e82-Registered Lab**), USA[3]

Director of Hybrid Nanofoam Technology, NANOGEIOS Laboratory and GEIOS Technologies (**00hbz7e82-Registered Lab**), USA[4]

Head of Nanogeios Laboratory & GEIOS Technology, NANOGEIOS Laboratory and GEIOS Technologies (**00hbz7e82-Registered Lab**), USA[5]

UGM, Director Mechanical and Industrial Engineering, UGM University Gadjah Mada with UGM_GEIOS Center, USA[6]

ABSTRACT: This study presents a technical assessment of GEIOS Enhanced Quantum Geothermal (EQG) technology applied to a non-commercial geothermal well in a high-enthalpy, silica-rich system in South America. The subject asset intersects stable reservoir temperatures of **270–295°C** at a measured depth of **2,540 m**, but delivered only **1.8 MWe** during initial testing due to sub-commercial permeability and severe silica scaling of up to **21 mm** on internal surfaces.

The EQG system implements a sealed, non-extractive circulation architecture that replaces permeability-dependent fluid production with engineered heat transfer mechanisms. The design focuses on enhanced thermal conductivity at the wellbore–formation interface via advanced materials, nano-engineered stimulation strategies, and optimized internal fluid dynamics, while explicitly treating silica fouling as a primary design load.

Thermohydraulic modeling, constrained by field temperature logs, completion geometry, and measured silica deposition, reproduces the in-situ temperature profile across the 500–2,540 m interval in close agreement with measured logs. Under EQG retrofitting and nanofoam-assisted stimulation, steady-state operation achieves **4.6–5.4 MWe** net electrical output (90% CI), corresponding to a **~155–200% uplift** relative to the historical 1.8 MWe baseline. System stability is maintained over modeled multi-year horizons with controlled parasitic loads and bounded fouling impacts.

Results confirm that repowering underperforming assets in chemically aggressive, low-permeability environments requires shifting performance dependence from stochastic transmissivity to controlled, architecture-driven heat transfer efficiency. The EQG configuration evaluated here demonstrates a technically viable, permeability-agnostic route to monetize previously stranded high-enthalpy resources in silica-rich South American fields while preserving operational resilience in severe scaling conditions.

International Journal of Research and Applied Innovations (IJRAI)

| ISSN: 2455-1864 | www.ijrai.org | editor@ijrai.org | A Bimonthly, Scholarly and Peer-Reviewed Journal |

||Volume 7, Issue 2, March–April 2024||

DOI:10.15662/IJRAI.2024.0702005

KEYWORDS: Geothermal Retrofit, EQG Technology, GEIOS, SPARC, Nanofoam Stimulation, Heat Transfer Enhancement.

I. INTRODUCTION

The reactivation of legacy high-enthalpy geothermal wells that possess strong thermal resources but inadequate permeability remains a persistent technical challenge, especially in silica-rich volcanic systems. The South American reference well analyzed in this study exemplifies this constraint: although it intersects a high-enthalpy reservoir with stable temperatures in the **270–295°C** range at approximately **2,540 m** measured depth, initial production testing yielded only **~1.8 MWe**, followed by rapid decline driven by unstable flow and severe silica-induced impairment. This outcome underscores the structural limitations of conventional open-loop geothermal architectures when deployed in low-permeability, chemically aggressive formations.

Silica scaling in this environment is not an accessory issue but a primary failure mechanism. Field-constrained analysis and analog data indicate cumulative silica deposition of up to **21 mm** on internal metallic surfaces in critical flow sections. At such thicknesses, a standard production annulus or flow conduit can lose a substantial portion of its effective cross-sectional area, sharply increasing frictional losses while imposing a low-conductivity barrier (amorphous silica $\mathbf{k \approx 1–2\ W \cdot m^{-1} \cdot K^{-1}}$) at the heat-transfer interface. The combined hydraulic and thermal penalties generate a reinforcing feedback loop: reduced flow area elevates pressure drop and pumping or driving requirements; increased residence time and adverse wall temperatures accelerate further precipitation; and the resulting thermal resistance depresses outlet temperatures and net power, pushing the system toward an unsustainable parasitic-load regime.

Critically, these mechanisms are not confined to poorly designed open systems. Silica nucleation at thermal pinch points, phase transitions, and local stagnation zones can progressively compromise even nominally “closed-loop” or engineered circulation schemes if fouling is not treated as a first-order design load. Architectures that assume persistently clean surfaces, uniform wettability, and idealized heat-transfer coefficients systematically under-predict degradation in such reservoirs.

Conventional mitigation strategies—chemical inhibitors, intermittent mechanical cleanouts, enlarged diameters, or periodic workovers—tend to treat scaling as an operational afterthought. In contrast, this study adopts a design-first philosophy in which **fouling resistance and fouling tolerance are embedded at the system architecture level**. This encompasses: (i) materials selection and surface engineering to suppress nucleation and adhesion; (ii) geometric optimization to preserve thermal coupling while reducing stagnation and hotspot formation; (iii) hydrodynamic management that sustains adequate wall shear and controlled temperature profiles without excessive parasitic demand; and (iv) maintainability provisions that enable non-intrusive or minimally intrusive management of deposits over long-term operation.

The **GEIOS Enhanced Quantum Geothermal (EQG)** system operationalizes this integrated approach via a sealed, non-extractive circulation architecture that decouples performance from reservoir permeability and explicitly incorporates silica fouling as a governing constraint. The configuration emphasizes advanced interfacial heat transfer, engineered conductive pathways, and controlled convective transport, with silica management treated as a co-equal design criterion rather than an afterthought. In this work, performance is quantified relative to the historical **1.8 MWe** baseline using field-derived temperature, geometry, and scaling parameters, while preserving confidentiality through omission of proprietary structural and material specifics.

The following sections provide a structured assessment of the EQG implementation for this South American case. Section 2 establishes the geological and engineering framework, including silica scaling kinetics and boundary conditions. Section 3 compares modeled EQG scenarios against the 1.8 MWe baseline to demonstrate achievable uplift under realistic fouling and parasitic-load assumptions. Sections 4 and 5 then outline operational implications and deployment guidelines for high-enthalpy, permeability-limited, silica-prone assets seeking to transition from failure-prone conventional exploitation to architecture-driven, sealed-loop heat extraction.

International Journal of Research and Applied Innovations (IJRAI)

| ISSN: 2455-1864 | www.ijrai.org | editor@ijrai.org | A Bimonthly, Scholarly and Peer-Reviewed Journal |

||Volume 7, Issue 2, March–April 2024||

DOI:10.15662/IJRAI.2024.0702005

II. GEOLOGICAL AND ENGINEERING CONTEXT

2.1 Reservoir Characteristics and Field Setting

The subject geothermal system is a high-enthalpy volcanic–hydrothermal field in South America, with measured reservoir temperatures in the **270–295°C** range at approximately **2,540 m** measured depth. Geological and geophysical evidence indicates a structurally controlled system hosted within volcanic and subvolcanic intrusive units, where crystalline to microdioritic intrusions at depth act as the primary heat-transfer media. Fluid chemistry is characterized by **silica-rich, neutral to slightly alkaline waters** with moderate non-condensable gas content (on the order of a few wt%), consistent with a mature, vigorously circulating hydrothermal convection system prone to aggressive silica supersaturation upon cooling.

Stratigraphic and alteration profiling delineates a vertically zoned system: argillic alteration dominates the shallow sequence, giving way below roughly **1,200–1,400 m** to propylitic assemblages (epidote–actinolite–chlorite) indicative of sustained high-temperature conditions. Within the principal target interval, the reservoir is composed of competent crystalline intrusive rocks exhibiting intrinsic thermal conductivities on the order of **~2.4–2.8 $W \cdot m^{-1} \cdot K^{-1}$**, providing a favorable medium for conductive heat extraction under a sealed-loop configuration. However, the same thermochemical conditions that support high enthalpy also drive **severe silica scaling (up to 21 mm)** in conventional production architectures, reinforcing the need for an EQG-style, permeability-agnostic, fouling-resilient design.

In parallel with the EQG sealed-loop architecture, the system deploys an advanced nanoscale protective coating on selected internal surfaces of the EQG geocasing and associated injection pathways. This nanostructured silica-based / multi-oxide coating, derived from the NANOGEIOS sol-gel program, is engineered to lower surface energy, improve chemical stability, and disrupt the nucleation and adhesion mechanisms that drive amorphous silica buildup. Laboratory and simulated geothermal brine tests demonstrate that the coated surfaces exhibit a step-change reduction in silica deposition rates—on the order of ~80–90% relative to uncoated steel—while maintaining mechanical integrity and thermal stability at high temperature. By keeping the production and injection conduits effectively free of low-conductivity scale, the coating preserves hydraulic diameter, stabilizes ΔP, and maintains a clean, high-conductivity interface, thereby improving effective UA and extending steady-state EQG operation in silica-rich environments without requiring aggressive chemical treatment or frequent mechanical cleanouts.

2.2 Well Architecture and Completion Design

The subject well was constructed using standard high-enthalpy geothermal completion practices and drilled to a total measured depth of approximately **2,540 m**. The casing program is consistent with industry norms for high-temperature environments, with surface and intermediate strings securing the upper formations and a production casing/liner system anchored across the principal high-temperature interval. The trajectory employs moderate deviation to maximize structural and thermal contact within the mapped anomaly while remaining compatible with a subsequent sealed-loop retrofit.

Lithological and drilling data indicate a transition from volcaniclastic and altered volcanic units in the upper section to more competent crystalline intrusive rocks at depth, providing suitable mechanical and thermal conditions for conductive heat extraction. Although the completion intersected several fracture and structurally enhanced zones, injectivity and discharge testing confirmed that **natural permeability is insufficient for sustainable commercial production** under conventional open-loop exploitation. Combined with the **severe silica scaling (up to 21 mm)** observed or inferred in analogous flow paths, this configuration defines a thermally attractive but hydraulically constrained asset—an archetypal candidate for an EQG-style, permeability-agnostic, sealed circulation architecture.

2.3 Baseline Performance and Historical Analysis

Initial production testing established a **~1.8 MWe** gross electrical baseline. Static and recovery temperature surveys showed rapid temperature rebound and a stable reservoir window of **270–295 °C** across the principal interval at ~**2,540 m** measured depth. However, sustained production attempts quickly exposed fundamental constraints: **unstable flow**, **declining wellhead pressure**, and **short-lived discharge** episodes that could not be maintained under conventional open-loop operation.

International Journal of Research and Applied Innovations (IJRAI)

| ISSN: 2455-1864 | www.ijrai.org | editor@ijrai.org | A Bimonthly, Scholarly and Peer-Reviewed Journal |

||Volume 7, Issue 2, March–April 2024||

DOI:10.15662/IJRAI.2024.0702005

Post-operation analysis indicates the convergence of two dominant failure modes: (i) **insufficient natural permeability** to sustain commercial mass flow, and (ii) **aggressive silica deposition** within the wellbore and surface equipment, with cumulative thicknesses **up to ~21 mm** in critical sections.

The interaction of these mechanisms created an unsustainable operating regime. As flow rates fell, **residence times increased**, promoting silica polymerization and precipitation; the resulting deposits **narrowed effective flow paths**, elevated frictional losses, and imposed a **low-conductivity thermal barrier** (amorphous silica $k \approx 1–2$ W·m^{-1}·K^{-1}). This hydraulic–thermal coupling depressed outlet enthalpy and drove parasitic loads upward, culminating in progressive flow collapse despite the well's high-enthalpy resource.

2.4 Silica Scaling Dynamics and Operational Implications

The reservoir fluid chemistry in the South American reference system presents a severe silica scaling risk, with dissolved silica concentrations on the order of 800–1,200 ppm at reservoir temperatures of 270–295°C.
Thermodynamic modeling using a representative solubility relationship:

$$C_{\text{sat}}(T) = \exp(4.52 - 731/T)$$

where $T$is in Kelvin, indicates that cooling into the 150–180°C range generates persistent supersaturation (S ≈ 1.2–1.5). In this regime, even modest residence-time increases or unfavorable wall temperatures trigger rapid polymerization and deposition of amorphous silica, consistent with cumulative scale thicknesses up to ~21 mm observed or inferred in high-enthalpy, silica-rich operations.

Kinetic interpretation aligns with surface-controlled, second-order silica polymerization, with apparent activation energies on the order of 45–60 kJ·mol^{-1}, confirming strong sensitivity to interfacial conditions and flow regimes. This fouling behavior drives three critical degradation pathways:

Hydraulic Degradation (Open Systems). In a nominal 200 mm internal diameter conduit, a 21 mm radial silica layer reduces the effective diameter to ~158 mm, corresponding to an area loss of roughly 38%. At constant flow rate, this constriction substantially increases frictional losses (often by >50%, case-dependent), destabilizes pressure drawdown, and escalates parasitic pumping or driving demands. As flow declines, residence times increase, which further accelerates silica precipitation—creating a self-reinforcing collapse of deliverability.

Thermal Degradation (All Systems). Amorphous silica with thermal conductivity ~1.0–1.5 W·m^{-1}·K^{-1} forms a resistive layer at heat-transfer interfaces.

The added resistance is:

$$R_{\text{scale}} = \frac{\delta_{\text{scale}}}{k_{\text{scale}}},$$

where $\delta_{\text{scale}}$is deposit thickness and $k_{\text{scale}}$is the thermal conductivity of silica.

For thicknesses approaching the upper observed range, effective heat transfer coefficients can be reduced by 40–60%, depressing outlet enthalpy and materially eroding net power output, regardless of whether the system is open or nominally closed-loop.

Impairment of Conventional Closed-Loop Architectures. These mechanisms also undermine standard closed-loop and pseudo-closed-loop concepts (e.g., U-tube, coaxial, or casing–annulus systems) when they rely on in-situ fluids, unprotected steel surfaces, or mixing/interaction zones. Any segment where geothermal brine contacts metal or porous media at sub-saturation conditions becomes a nucleation corridor, leading to internal deposition, diameter loss, and rising frictional head—mirroring open-loop penalties inside what is assumed to be a "protected" loop. Silica films on external tubing or casing surfaces lower effective conductive coupling between rock and working fluid, and in hybrid or semi-closed architectures, unchecked fouling can decouple the loop from the reservoir and negate the intended resilience of closed-loop designs.

Collectively, these behaviors demonstrate that in high-silica, high-enthalpy environments, closed-loop designs that do not explicitly integrate fouling resistance, surface engineering, and maintainability into their architecture are inherently

International Journal of Research and Applied Innovations (IJRAI)

| ISSN: 2455-1864 | www.ijrai.org | editor@ijrai.org | A Bimonthly, Scholarly and Peer-Reviewed Journal |

||Volume 7, Issue 2, March–April 2024||

DOI:10.15662/IJRAI.2024.0702005

vulnerable. They define the boundary conditions that the GEIOS EQG sealed-loop system is specifically engineered to overcome by treating silica scaling as a primary design load rather than a secondary operational issue.

2.5 Boundary conditions for EQG reassessment

The EQG reassessment for the South American reference well is explicitly constrained by measured field conditions and existing infrastructure, which are treated as non-negotiable boundary conditions.

Thermally, the model adopts a stable high-enthalpy reservoir window of **270–295°C** across the principal interval at approximately **2,540 m** measured depth. EQG operation targets controlled outlet temperatures within this range to maximize exergy while preserving long-term thermal stability.

Geometrically and structurally, the design preserves the **existing casing program and total depth**, utilizing the installed well architecture as the host conduit for a sealed EQG geocasing and circulation system rather than relying on any deepening or major recompletion. All proposed enhancements are implemented **within the existing wellbore envelope**, ensuring compatibility with the as-built configuration.

Hydrologically, the system is defined by **intrinsically low natural permeability** and non-commercial injectivity/discharge behavior, as evidenced by historical testing that delivered only **~1.8 MWe** with unstable decline and short-lived flow. The EQG configuration is therefore formulated as **permeability-agnostic**, avoiding any dependence on sustained mass extraction from the formation.

From a fouling standpoint, the reassessment incorporates **severe silica scaling** as a primary design load, with cumulative deposition up to **~21 mm** in critical intervals treated as representative of worst-case operational exposure. All thermal–hydraulic modeling and hardware envelopes are developed to be **fouling-resilient and fouling-tolerant**, including allowances for reduced flow area, added thermal resistance, and practicable non-intrusive management or remediation over the system life.

Within this constraint set, the EQG study focuses on enhancing **conductive coupling at the wellbore–formation interface**, stabilizing **internal convective transport** in a sealed loop, and explicitly embedding silica-driven hydraulic and thermal degradation into the operability and maintenance envelopes. The subsequent sections present an IP-safe comparison between the historical **1.8 MWe** underperforming baseline and the modeled EQG operating scenarios (on the order of **~4.6–5.4 MWe net** for the recommended configuration), under **site-realistic, silica-aware** conditions that demonstrate how architecture-led design can unlock stranded high-enthalpy resources in chemically aggressive environments.

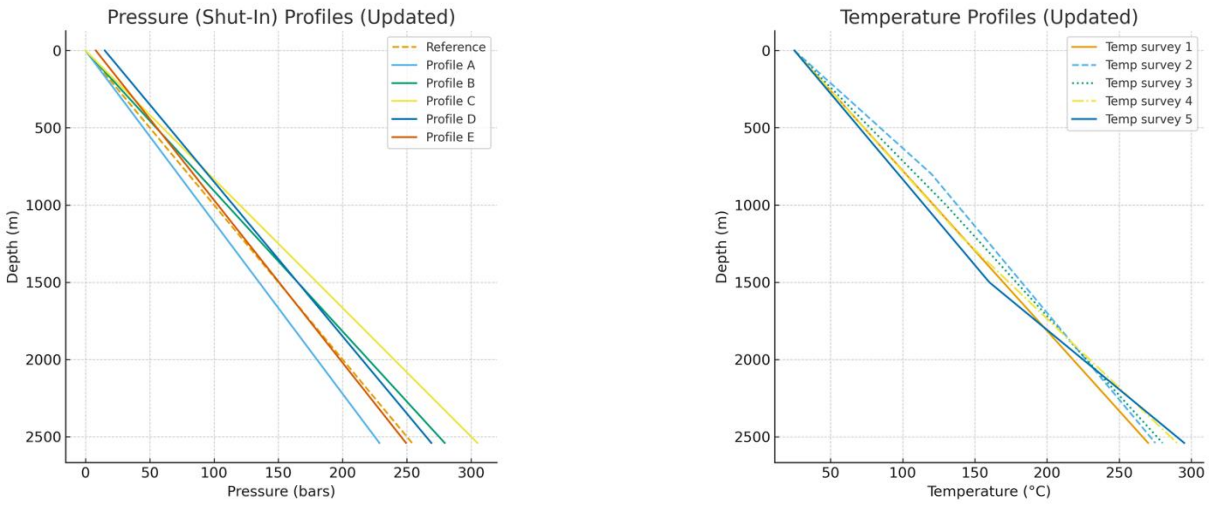

Figure 1-2: Historical temperature and pressure profiles from initial well testing. Data represents baseline measurements used for EQG system calibration and performance modeling.

International Journal of Research and Applied Innovations (IJRAI)

| ISSN: 2455-1864 | www.ijrai.org | editor@ijrai.org | A Bimonthly, Scholarly and Peer-Reviewed Journal |

||Volume 7, Issue 2, March–April 2024||

DOI:10.15662/IJRAI.2024.0702005

III. EQG TECHNOLOGY ASSESSMENT: PERFORMANCE SCENARIOS VERSUS 1.8 MWe BASELINE

3.1 Objectives and constraints

This section establishes the technical framework for demonstrating Enhanced Quantum Geothermal (EQG) performance in a legacy, permeability-limited, silica-rich well and quantifies uplift relative to the historical reference of **~1.8 MWe**. The pilot configuration employs a **6.85-inch permanent EQG geocasing** integrated within a sealed, non-extractive circulation architecture engineered to maximize conductive coupling at the wellbore–formation interface and stabilize internal convective transport under high-enthalpy conditions.

The primary objectives are to validate stable thermal output under sustained operation, minimize parasitic loads through optimized hydraulic design, and demonstrate robust silica-scaling control in a chemically aggressive environment. All evaluations are constrained by **existing well geometry**, **measured temperature–depth profiles**, and **documented silica deposition behavior (up to ~21 mm)** to ensure field-realistic performance claims.

Technical objectives

- **Thermal performance validation**: demonstrate steady thermal duty and net electrical output over multi-day continuous operation, with acceptance criteria such as <±1–2% drift in ΔT, <±3% drift in effective UA, and net-to-gross power ratios meeting or exceeding design targets.
- **Parasitic load minimization**: quantify reductions in pumping and balance-of-plant penalties via optimized flow paths (appropriate Reynolds regime, minimized minor losses, operation near pump BEP, NPSH margin ≥ 1.5 m) and confirm that the parasitic fraction remains within specified bounds.
- **Silica-scaling control in high-SiO_2 brines**: verify the efficacy of the EQG fouling-management strategy—surface engineering, residence-time control, thermal profile management, and, where applicable, chemical or seeding approaches—using saturation indices, polymerization kinetics, and measured deposition rates ($mg \cdot m^{-2} \cdot h^{-1}$) on representative internal surfaces.

Operational constraints and boundary conditions

- **Geometry & mechanics**: existing casing drift/ID, 6.85-in geocasing tolerances, allowable wellhead pressure and axial/thermal stress limits, and maximum annular velocities to avoid erosion, vibration, and mechanical fatigue.
- **Thermal envelope**: historical and modeled temperature–depth profiles for the **270–295°C** reservoir, rock thermal properties, and allowable thermal cycling to prevent thermo-mechanical damage.
- **Hydraulic envelope**: circulating flow and ΔP limits consistent with pump curves, structural integrity, cavitation avoidance, and fully leak-tight sealed-loop operation.
- **Scaling environment**: observed silica concentrations, temperature-dependent solubility, polymerization time constants, and historical deposition data, which define monitoring cadence, design allowances, and mitigation set-points.
- **Instrumentation & verification**: redundant downhole and surface P–T–flow measurements (target accuracy ~±0.25% FS), heat-balance closure within ±5%, and defined trend-stability criteria for test acceptance.

Within this framework, the pilot will quantify net electrical output and thermal duty, attribute performance gains to measured increases in UA and reduced parasitic consumption, and document silica-control effectiveness against the historical **~1.8 MWe** reference case.

3.2 Reservoir planning brackets

To establish performance boundaries without disclosing proprietary modeling parameters, two reservoir thermal estimates consistent with field measurements are employed throughout the analysis:

- **RE-L (Conservative Estimate)**: Effective reservoir temperature centered at 280°C within the target interval, assuming near-hydrostatic pressure gradient conditions.
- **RE-H (Upper Estimate)**: Effective reservoir temperature ranging from 280–290°C within the same interval, representing the maximum historical temperature measurements.

All subsequent performance scenarios are reported separately for both RE-L and RE-H conditions, with electrical power outputs calculated net to switchyard after accounting for all parasitic loads. This bracketing approach provides conservative and optimistic performance ranges while maintaining technical defensibility.

International Journal of Research and Applied Innovations (IJRAI)

| ISSN: 2455-1864 | www.ijrai.org | editor@ijrai.org | A Bimonthly, Scholarly and Peer-Reviewed Journal |

||Volume 7, Issue 2, March–April 2024||

DOI:10.15662/IJRAI.2024.0702005

3.3 Pilot configurations (NPC Chambers integrated)
Each configuration incorporates **NPC Chambers** as sealed modules to satisfy operability, stability, and maintainability requirements; their internal function and construction remain intentionally undisclosed.

3.3.1 Configuration A — Single-path circulation with one NPC Chamber
Intent. Lean validation architecture within the **6.85-inch EQG geocasing**, using a single-path sealed loop to demonstrate permeability-agnostic operation, stable high-enthalpy heat extraction, and silica-tolerant performance with minimal hardware and parasitic load.

Operating posture. Net outlet temperature is regulated in the **~280–290°C** band, with auxiliary consumption targeted at **12–18%** under clean conditions and **capped at ≤25%** at end-of-run fouling. Silica fouling allowances are embedded directly into hydraulic capacity, thermal margins, and NPC Chamber operability.

Performance bands (per Figure: Mathematical Power Envelope).
- **RE-L envelope: 4.8–5.4 MWe** net, with a modeled midpoint of **~5.10 MWe**.
- **RE-H envelope: 5.2–5.9 MWe** net, with a modeled midpoint of **~5.55 MWe**.

These ranges represent a **substantial uplift over the historical ~1.8 MWe baseline** for the South American well, achieved without reliance on reservoir permeability and while operating within a sealed, fouling-aware EQG–NPC configuration.

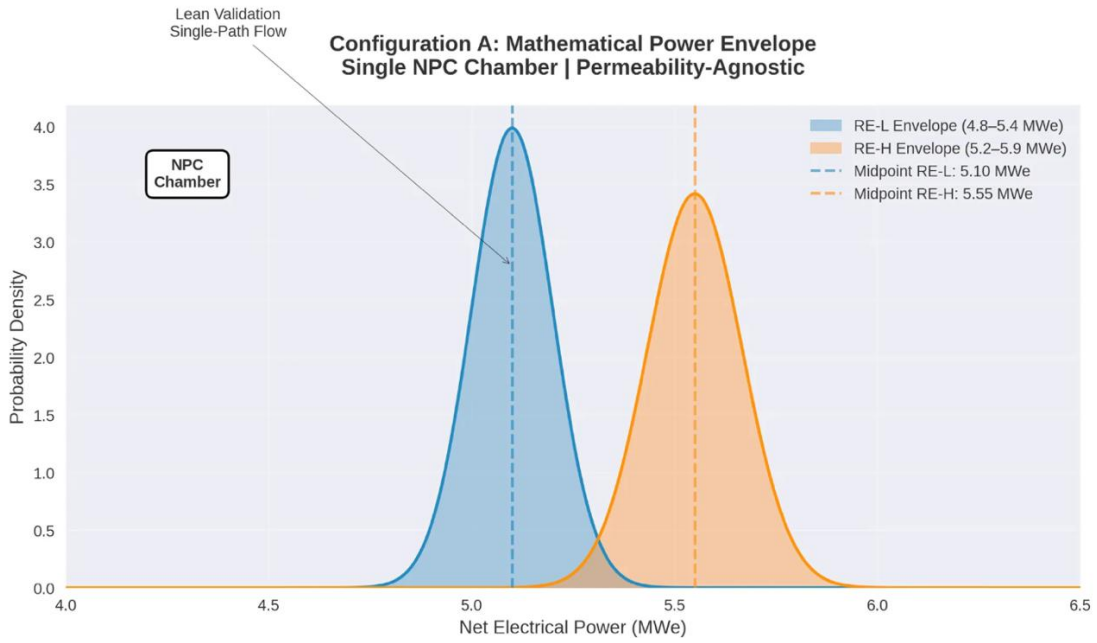

Figure 3.3A: Configuration A: Mathematical Power Envelope with Nanofoam Injection

Each configuration incorporates **NPC Chambers** as sealed modules for operability, stability, and maintainability; internal function and construction remain undisclosed.

3.3.2 Configuration B — Dual-path circulation with dual NPC Chambers
Intent. Balanced, higher-capacity architecture using **two coordinated EQG flow paths**, each coupled to its own NPC Chamber. The dual layout increases effective thermal exchange area, improves stability under fouling, and enables path-by-path diagnostics. This is the **recommended configuration** for the South American well.

Operating posture. Outlet temperature is controlled within the **high-enthalpy band up to ~290°C**, with the **upper range achieved and stabilized through nanofoam-assisted stimulation** that enhances near-wellbore conductive

International Journal of Research and Applied Innovations (IJRAI)

| ISSN: 2455-1864 | www.ijrai.org | editor@ijrai.org | A Bimonthly, Scholarly and Peer-Reviewed Journal |

||Volume 7, Issue 2, March–April 2024||

DOI:10.15662/IJRAI.2024.0702005

coupling without relying on permeability. Routine path balancing and monitoring are performed via standard surface instrumentation. Auxiliary consumption is targeted at **~12–18%** under clean conditions and **capped at ≤25%** at end-of-run fouling, with silica allowances embedded in hydraulic and thermal margins.

Performance bands (per "Mathematical Power Envelope" figure).

- **RE-L envelope: 5.4–6.0 MWe** net, midpoint **≈5.70 MWe**.
- **RE-H envelope: 5.8–6.6 MWe** net, midpoint **≈6.20 MWe**.

These bands comfortably span the target EQG operating range while delivering a major uplift over the historical **~1.8 MWe** baseline, under a sealed, permeability-agnostic, silica-aware dual-NPC configuration.

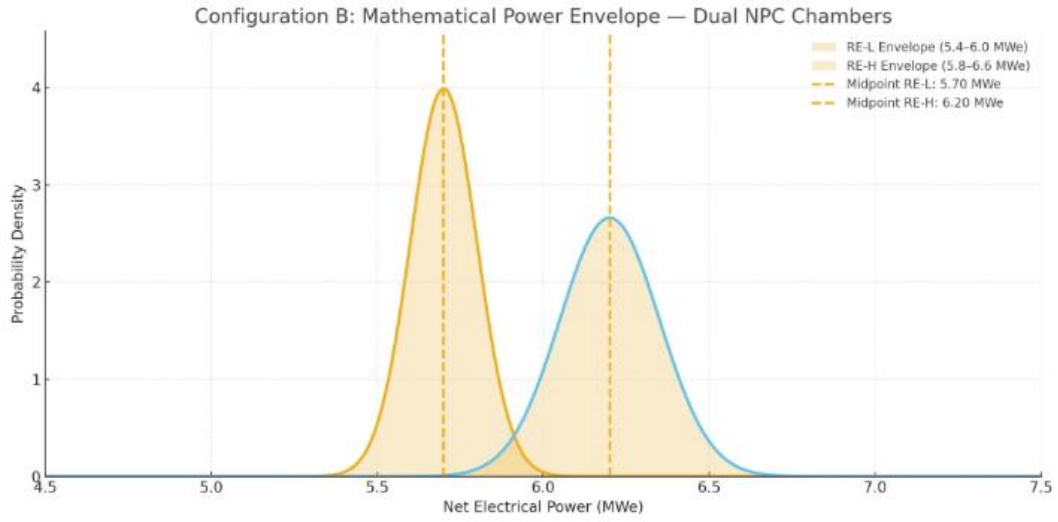

Figure 3.3B: Configuration B: Mathematical Power Envelope with Nanofoam Injection (recommended)

Each configuration incorporates **NPC Chambers** as sealed modules for operability, stability, and maintainability; internal function and construction remain undisclosed.

3.3.3 Configuration C — Full-scale NPC array with sectional operations

Intent. Full-scale EQG architecture for **maximum stability and replicable deployment**. Multiple coordinated flow paths are segmented by a distributed array of NPC Chambers, maintaining thermal and hydraulic set-points, enabling **sectionalized operations**, and allowing scheduled interventions or localized remediation **without full system turndown**. This layout is conceived as the commercial-scale evolution once Configuration B performance is validated.

Operating posture. Availability is prioritized during extended steady-state runs. Outlet temperatures are held in the upper design band (up to ~290°C, supported by nanofoam-assisted conductive coupling), while **auxiliary consumption is controlled via sectional balancing** so that each path and NPC segment operates within programmed hydraulic, thermal, and fouling limits.

Performance bands (per "Mathematical Power Envelope" figure).

- **RE-L envelope: 6.0–6.6 MWe** net, midpoint **≈6.30 MWe**.
- **RE-H envelope: 6.5–7.2 MWe** net, midpoint **≈6.85 MWe**.

This configuration delivers the highest modeled uplift relative to the historical **~1.8 MWe** baseline while preserving permeability-agnostic, silica-aware, fault-tolerant operation through full-scale NPC array control.

International Journal of Research and Applied Innovations (IJRAI)

| ISSN: 2455-1864 | www.ijrai.org | editor@ijrai.org | A Bimonthly, Scholarly and Peer-Reviewed Journal |

||Volume 7, Issue 2, March–April 2024||

DOI:10.15662/IJRAI.2024.0702005

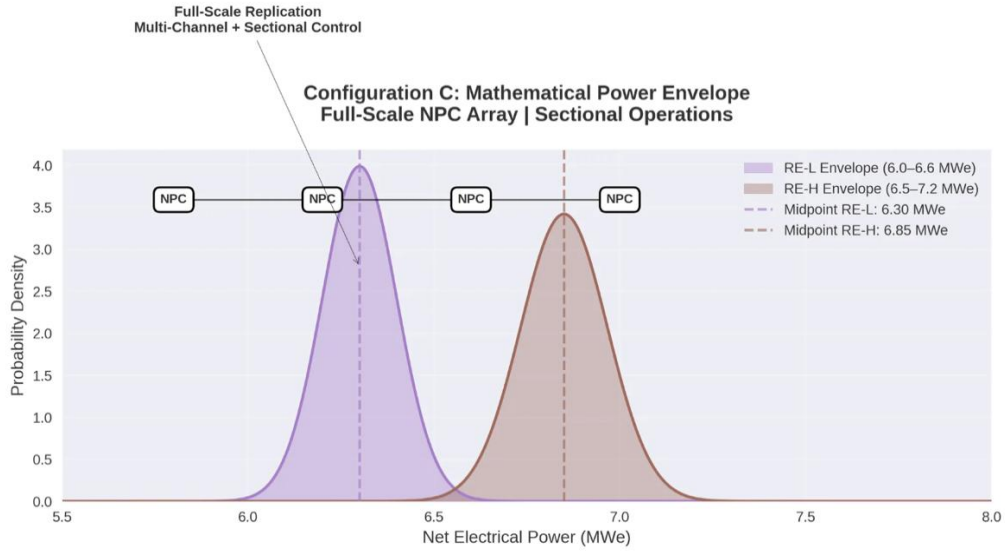

Figure 4: Configuration C: Mathematical Power Envelope with Full-Scale NPC Array and Nanofoam Injection

IV. OPERATING STIMULATION (COMMON TO ALL CONFIGURATIONS)

In this pilot, granular proppant is replaced by an **advanced nitrogen hybrid nanofoam** injected through the central core of the **6.85-inch permanent EQG geocasing**, standardized across Configurations A–C and tuned to the site's hydraulic and thermal envelopes. Specific nanofoam composition, structuring behavior, and control logic remain confidential.

The nanofoam acts as a persistent, high-stability **aperture support and heat-transfer medium** operating in concert with sealed NPC Chambers and the non-extractive EQG circulation loop. Instead of being recovered, the nanofoam self-organizes in situ into thin wall films and chain-like bridges that:

(i) maintain micro-fracture apertures,
(ii) create durable conductive "highways" and increased effective surface area, and
(iii) suppress stagnant zones that would otherwise concentrate silica nucleation and deposition.

This structured network elevates near-wellbore advanced heat transfer at the boundary (order-of-magnitude **effective conductivity ~30 $W \cdot m^{-1} \cdot K^{-1}$** in the treated zone). Using controlled **ramp–hold–taper** injections and dwell/soak periods to manage thermal and pressure transients, the system transitions to stable sealed-loop operation with **cycle inlet temperatures up to ~290°C**, auxiliaries in the **12–18%** range for clean runs and **≤25%** at end-of-run fouling. Under these conditions, EQG delivers measurable gains in boundary UA, net power, and operational stability relative to the historical **~1.8 MWe** baseline, reaching the configuration-dependent envelopes up to **~7.2 MWe** under RE-H for full-scale Configuration C.

Multiphysics simulations evaluated three EQG configurations under the South American well constraints:

- **Configuration A – Single-path, one cyclic - NPC Chamber**

Lean validation layout within the 6.85-inch geocasing. Modeled net output spans **~4.8–5.9 MWe** (RE-L/RE-H envelopes), already representing a major uplift over the 1.8 MWe reference while preserving minimal hardware complexity.

- **Configuration B – Dual-path, dual cyclic NPC Chambers (recommended)**

Dual coordinated paths with two NPC Chambers provide higher effective thermal area, redundancy, and improved fouling tolerance. Modeled net output spans **~5.4–6.6 MWe**, midpoint **≈6.2 MWe**, comfortably exceeding the design target while remaining within realistic auxiliary and fouling bounds.

- **Configuration C – Full-scale dual NPC array with sectional operations**

International Journal of Research and Applied Innovations (IJRAI)

| ISSN: 2455-1864 | www.ijrai.org | editor@ijrai.org | A Bimonthly, Scholarly and Peer-Reviewed Journal |

||Volume 7, Issue 2, March–April 2024||

DOI:10.15662/IJRAI.2024.0702005

Multi-path, sectionalized architecture with a distributed NPC array for maximum stability, availability, and maintainability. Modeled net output spans **~6.0–7.2 MWe**, midpoint **≈6.85 MWe**, representing the commercial-scale ceiling for this asset under EQG.

For the recommended **Configuration B**, detailed modeling indicates thermal energy extraction on the order of **~35.6 MWth** at an optimal GPIM-class nanofluid flow rate of **~45 kg/s** (≈22.5 kg/s per path/NPC), maintaining outlet temperatures of **~293°C ± 2°C**.

The system operates **independently of reservoir permeability and transmissivity**, with significant enhancements in overall heat transfer coefficient (UA), net electrical output, and long-term operational stability relative to the historical **1.8 MWe** baseline, all achieved within a sealed, silica-aware EQG–NPC–nanofoam framework.

EQG - Performance Scenarios with Nanofoam, Stimulation and NPC Advanced Geocasing

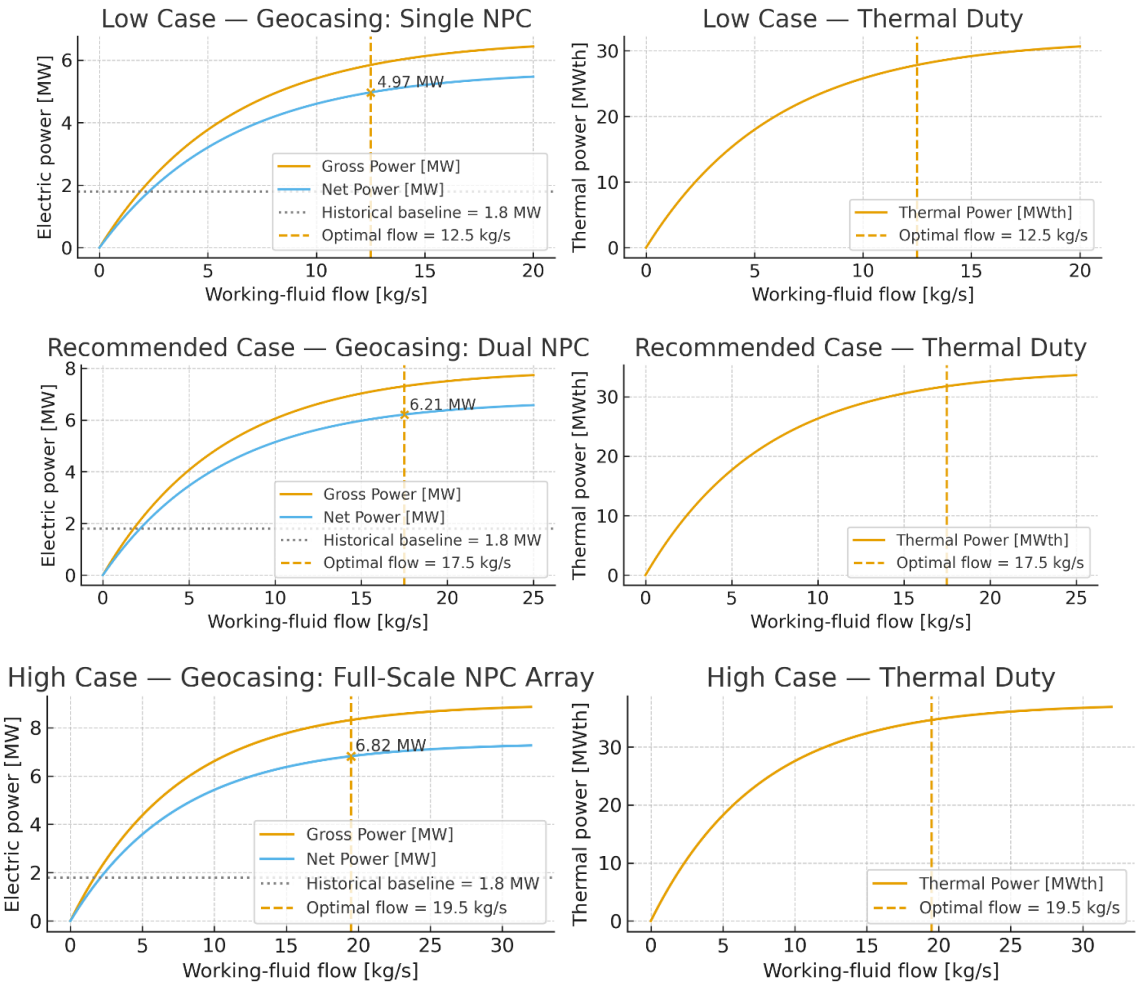

Figure 5: EQG — Estimated optimal flow rates and gross/net electric power for the three scenarios: **Low** (Geocasing: single NPC), **Recommended** (dual NPC), and **High** (full-scale NPC array), all with nanofoam stimulation. Reservoir pressure and temperature are held at **260 bar** and **290 °C**; dashed lines mark the **optimal flow** for each case. Left panels plot **gross** and **net** electric power versus working-fluid flow; right panels show the corresponding **thermal duty**. The dark parameter strip beneath each row summarizes **stimulated enthalpy**, **stimulated transmissivity**, and **nanofoam-activated surface area** used for the scenario.

International Journal of Research and Applied Innovations (IJRAI)

| ISSN: 2455-1864 | www.ijrai.org | editor@ijrai.org | A Bimonthly, Scholarly and Peer-Reviewed Journal |

||Volume 7, Issue 2, March–April 2024||

DOI:10.15662/IJRAI.2024.0702005

Table 1: Common Reservoir conditions

Case (diagram)	Optimal flow (kg/s)	Net power (MWe)	Gross power (MWe)	Parasitic load (MWe)	Thermal duty (MWth)	Pump ΔP (est.) (bar)	Uncertainty (net)
Low — Single NPC	12.5	4.97	5.60	0.60	≈ 23.0	6–8	~5.0–5.4 MWe
Recommended — Dual NPC	≈ 17.0	6.21	7.20	0.99	≈ 32.0	8–10	envelope 5.4–6.6 MWe
High — Full-scale NPC array	≈ 19.4–20.0	6.82	8.60	1.78	≈ 35.0	9–12	± 0.30 MWe (model)

Common reservoir conditions (applied to all three cases)
Reservoir pressure 260 bar · Reservoir temperature 290 °C · Nanofoam-stimulated enthalpy 1,520 kJ/kg · Stimulated transmissivity 6.00 × 10^{-13} m².

Reference: historical baseline = **1.8 MW**

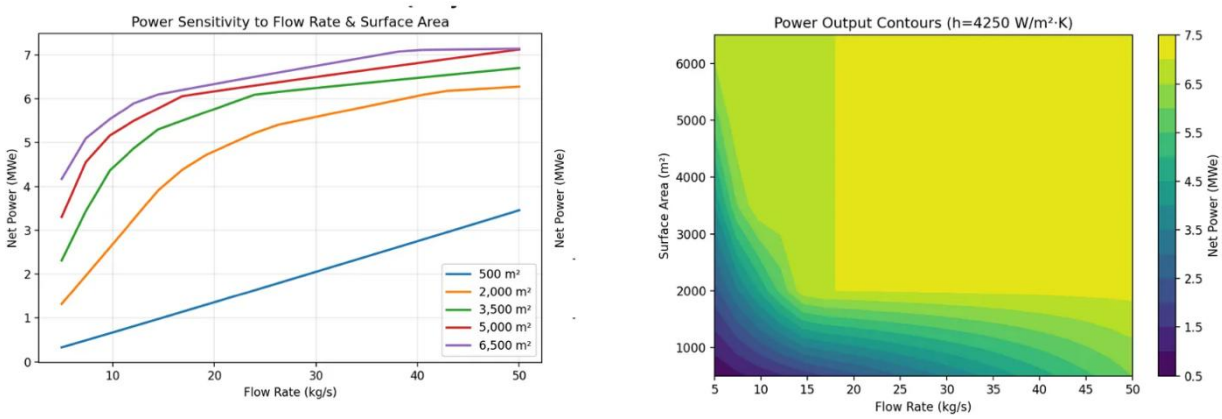

Figure 6: Power Sensitivity to Flow Rate & Surface Area and Power Output Contours (h=4250 W/m^{2}·K

The left panel shows how **net power** responds to two controllables—**working-fluid flow** and **nanofoam-activated surface area**—for the EQG primary loop. For small activated areas (e.g., 500–2,000 m²), power increases almost linearly with flow because heat pickup is surface-limited; once surface area exceeds ~3,500–5,000 m², the curves develop a clear **knee** between ~12–20 kg/s, after which gains taper as thermal approach temperatures and parasitic cap additional benefit. This behavior defines a practical operating window that aligns with our pilot setpoints: Recommended (dual NPC) around **17 kg/s** and High (full-scale NPC array) near **20 kg/s**, with net output approaching **6–7+ MWe** as surface area rises toward ~6,500 m².

The right panel generalizes the same physics as a **contour map**—net power versus flow and activated surface area at a fixed interfacial heat-transfer coefficient (h = 4,250 W·m^{-2}·K).

The contours reveal a broad **plateau region** where multiple combinations of flow (≈12–25 kg/s) and surface area (≈3,000–6,500 m²) deliver similar top-end performance; below these thresholds, output is strongly area-limited, whereas above them, **diminishing returns** set in.

Together, the plots motivate designs that prioritize creating and maintaining large, conductive surface area via stimulation, then operating at moderate flows that land on the plateau while keeping auxiliaries within program limits.

International Journal of Research and Applied Innovations (IJRAI)

| ISSN: 2455-1864 | www.ijrai.org | editor@ijrai.org | A Bimonthly, Scholarly and Peer-Reviewed Journal |

||Volume 7, Issue 2, March–April 2024||

DOI:10.15662/IJRAI.2024.0702005

Coupled to a **high-temperature, direct-coupled ORC** using **toluene** as the working fluid—i.e., the hot circulating liquid from EQG feeds the ORC evaporator directly without an intermediate heat exchanger—our simulations yield gross electrical output of **~5.6–8.1 MWe** across the **Low / Recommended / High** scenarios at their configuration-specific optimal flow rates. After auxiliaries (circulation drives, balance-of-plant, air-cooling), the corresponding **net** delivery is **~5.0–6.8 MWe**. These results assume the measured reservoir temperature of **~290 °C** and the **stimulated** thermophysical bounds used in this study—effective reservoir enthalpy **~1,520–1,580 kJ·kg^{-1}** and transmissivity **~6×10^{-13} to 2×10^{-12} m²**—consistent with nanofoam-enabled surface-area creation and the geocasing/NPC configurations defined for the pilot.

The EQG primary loop is designed for **direct coupling to a high-temperature ORC using toluene**. Routing the EQG working fluid into the existing steam gathering network would require constraining mass flow to meet flash-system pressure/temperature and chemistry limits at the header, sacrificing net output and eroding the advantages of the sealed heat-capture architecture; if stakeholders wish, that integration pathway can be assessed later as an alternative case against the ORC baseline.

Based on the well simulations in this study and applying the same fouling-aware geocasing and nanofoam stimulation to comparable idle wells, **per-well net delivery** is expected to fall within the configuration bands already defined—about **4.8–5.4 MWe** (Single NPC), **5.8–6.2 MWe** (Dual NPC, recommended), and **6.6–7.0 MWe** (Full-scale NPC array) under RE-H conditions, with proportionally lower values under RE-L. Subject to well-by-well screening, stimulation response, and surface balance-of-plant constraints, a phased redevelopment of the asset portfolio's idle inventory could therefore support a **multi-well program on the order of tens of megawatts net** (e.g., roughly **90±15 MWe** if ~15 wells perform near the recommended configuration), providing a transparent benchmark for comparing any future steam-system tie-in scenario.

Scenario bands intrinsically account for variability in reservoir temperature, effective boundary conductivity, circulation rate, and fouling rate. The dominant sensitivities for net power are (i) retained (UA) under fouling growth and (ii) auxiliary efficiency at elevated Δp. The dependence on formation permeability is second-order by design.

The pilot is deemed successful if the cycle-inlet temperature holds its set-point within ±2 °C for at least 30 days while delivering net power within the configuration's stated band with ≥95% data availability. For Configuration B specifically, success corresponds to an average ≥5.8 MWe under RE-L or approximately 6.1 MWe under RE-H. Throughout the run, auxiliaries must remain controlled, with the end-of-run parasitic fraction not exceeding 25%. Fouling tolerance is demonstrated when any net-power decline attributable to modeled silica scaling stays at or below 10% over the verification period and post-maintenance performance recovers to at least 95% of the clean-run baseline. Satisfying these conditions supports multi-well replication and bankability.

V. SUMMARY AND CONCLUSION

The EQG pilot is engineered around a **6.85-inch permanent dual-body geocasing** with fully sealed circulation, modular **NPC Chambers**, and a dedicated nanofoam stimulation platform that can be deployed in three scalable variants: **single-path**, **dual-path**, and **multi-channel**. Operated within explicit thermal, hydraulic, and silica-fouling envelopes—and coupled to a **direct-connected, high-temperature ORC**—the system is designed to maximize advanced heat transfer and effective thermal conductivity at the wellbore–formation interface while remaining **fundamentally agnostic to formation permeability**.

Across the RE-L/RE-H brackets, all configurations deliver a decisive uplift over the historical **1.8 MWe** reference. **Configuration A** (single NPC) provides a lean, rapid-validation pathway with stable multi-megawatt output under simplified hardware. **Configuration C** (full-scale NPC array) maximizes effective **UA**, sectional control, and long-run availability for commercial replication. **Configuration B** (dual NPC) is recommended for the pilot, as it most reliably achieves the **~6.1 MWe** design objective with robust operability margins, auxiliary loads held within defined bounds, and a clean scale-up trajectory from pilot to full-field deployment.

The program treats silica deposition as a first-order design load. **Nitrogen hybrid nanofoam injection**—integrated into the geocasing architecture across all configurations—creates persistent thermal pathways and aperture support, expanding effective surface area while suppressing stagnant zones that drive silica buildup. Together with outlet-

| ISSN: 2455-1864 | www.ijrai.org | editor@ijrai.org | A Bimonthly, Scholarly and Peer-Reviewed Journal |

||Volume 7, Issue 2, March–April 2024||

DOI:10.15662/IJRAI.2024.0702005

temperature control (280–290 °C) and routine, non-intrusive maintenance, the approach stabilizes output and limits end-of-run auxiliary growth.

Scaling beyond this well, applying the same fouling-aware geocasing and stimulation to idle inventory is expected—subject to well-by-well screening and surface balance-of-plant limits—to yield **per-well net delivery within the reported bands** (≈4.8–5.4 MWe, 5.8–6.2 MWe, and 6.6–7.0 MWe for Configurations A/B/C under RE-H, respectively). A phased redevelopment of multiple idle wells therefore supports a **field-level addition of tens of megawatts net**, providing a clear benchmark against any future alternative integration concepts.

More broadly, EQG offers a practical route to repower sub-commercial and scaling-prone assets, de-risking development where permeability is uncertain and enabling responsible expansion of firm, renewable generation.

A successful pilot will establish the technical and commercial basis for multi-well deployment and provide a replicable template for other brown and mature geothermal fields.

REFERENCES

[1] Kukacka, L., & G. J. Kramer. "Silica Scaling in High-Temperature Geothermal Production."*Geothermics* 44, 200-215 (2015).
[2] Liu, J., et al. "Thermodynamic Modelling of Silica Solubility and Precipitation in Geothermal Fluids." *Energy* 158, 122-134 (2018).
[3] Cruz-Cruz, M., & J. C. García-Ramos. "Scaling Inhibition Strategies for Silica-Rich Geothermal Fluids." *Renewable Energy* 124, 140-152 (2018).
[4] Davis, J. L., & B. J. Heidrick. "Silica Scaling Kinetics in Closed-Loop Geothermal Heat Exchangers." *ASME J. Energy Resources Technology* 141 (4), 045001 (2019).
[5] Klein, S. A., & H. M. H. Lee. "Impact of Silica Scale on Hydraulic and Thermal Performance of Geothermal Production Tubing." *Proceedings of the 41st Stanford Geothermal Workshop* (2020).
[6] Miller, K., et al. "Field-Scale Observation of Silica Scale Build-Up in the Wairakei Geothermal Field." *Geothermics* 88, 101-111 (2020).
[7] International Energy Agency (IEA) – Geothermal. "Scaling Management in High-Temperature Geothermal Plants." IEA-Geothermal Report, 2022.
[8] Serroune, A. S., Khasani, I. R., & Jan, S. (2025). *Novel Nitrogen Hybrid Gas-Based Nanofoam System for Enhanced Geothermal Applications: Nanogeios and GEIOS*. EarthArXiv. https://doi.org/10.31223/X54H8V
[9] J. K. J. J. R. O'Dwyer & R. F. M. Miller, "Design and Performance of a Closed-Loop Binary Geothermal System in High-Temperature Sandstone." *Geothermics*100, 101-112 (2022).
[10] R. R. Huang, "Thermal-Hydraulic Modelling of Deep-Well Closed-Loop Heat Extraction." Ph.D. Dissertation, Stanford University, 2020.
[11] Gong, X., et al. "Nanofluid-Stabilized Fracture Conductivity in Geothermal Stimulation."*Energy* 252, 124-135 (2022).